Heliyon 10 (2024) e33885

Contents lists available at ScienceDirect

Heliyon

journal homepage: www.cell.com/heliyon

Research article

Development and validation of Mayaro virus with luciferase reporter genes as a tool for antiviral assays

Mikaela dos Santos Marinho [a,1], Ya-Nan Zhang [b,1], Natasha Marques Cassani [a], Igor Andrade Santos [a], Ana Laura Costa Oliveira [a], Anna Karla dos Santos Pereira [c], Pedro Paulo Corbi [c], Bo Zhang [b,**], Ana Carolina Gomes Jardim [a,d,*]

[a] *Laboratory of Antiviral Research, Institute of Biomedical Science, Federal University of Uberlândia (UFU), Uberlândia, MG, Brazil*
[b] *Key Laboratory of Virology and Biosafety, Wuhan Institute of Virology, Chinese Academy of Sciences, Wuhan, 430071, China*
[c] *Institute of Chemistry, University of Campinas (UNICAMP), Campinas, SP, Brazil*
[d] *Institute of Biosciences, Humanities, and Exact Sciences, São Paulo State University (UNESP), Campus, São José do Rio Preto, SP, Brazil*

ARTICLE INFO

Keywords:
Mayaro virus
Reporter virus
Zika virus
Antiviral
Rimantadine hydrochloride

ABSTRACT

Arboviruses are etiological agents in an extensive group of emerging diseases with great clinical relevance in Brazil, due to the wide distribution of their vectors and the favorable environmental conditions. Among them, the Mayaro virus (MAYV) has drawn attention since its emergence as the etiologic agent of Mayaro fever, a highly debilitating disease. To study viral replication and identify new drug candidates, traditional antiviral assays based on viral antigens and/or plaque assays have been demonstrating low throughput, making it difficult to carry out larger-scale assays. Therefore, we developed and characterized two DNA-launched infectious clones reporter viruses based on the MAYV strain BeAr 20290 containing the reporter genes of *firefly luciferase (FLuc)* and *nanoluciferase (NLuc),* designated as MAYV-*firefly* and MAYV-*nanoluc*, respectively. The viruses replicated efficiently with similar properties to the parental wild-type MAYV, and luminescence expression levels reflected viral replication. Reporter genes were also preserved during passage in cell culture, remaining stably expressed for one round of passage for MAYV-*firefly* and three rounds for MAYV-*nanoluc*. Employing the infectious clone, we described the effect of Rimantadine, an FDA-approved Alzheimer's drug, as a repurposing agent for MAYV but with a broad-spectrum activity against Zika virus infection. Additionally, we validated MAYV-*nanoluc* as a tool for antiviral drug screening using the compound EIDD-2749 (4′-Fluorouridine), which acts as an inhibitor of alphavirus RNA-dependent RNA polymerase.

1. Introduction

Arboviruses make up an extensive group of emerging pathogens of great clinical relevance in Brazil, due to the wide distribution of their vectors, mediated by favorable environmental conditions [1]. Although their circulation is geographically restricted by vectors

* Corresponding author. Institute of Biomedical Science, ICBIM/UFU, Avenida Amazonas, Bloco 4C – sala 216, Umuarama, Uberlandia, MG, CEP: 38405-302, Brazil.
** Corresponding author.
E-mail addresses: zhangbo@wh.iov.cn (B. Zhang), jardim@ufu.br (A.C.G. Jardim).
[1] These authors contributed equally to this work.

https://doi.org/10.1016/j.heliyon.2024.e33885
Received 12 June 2024; Accepted 28 June 2024
Available online 2 July 2024

and reservoir hosts, arboviruses have the potential to adapt to infect new organisms, spreading beyond the endemic areas [2]. In this sense, the global emergence and resurgence of those pathogens lead to management and preparedness efforts for possible new outbreaks, including the search for antivirals against them [3].

Mayaro virus (MAYV; specie *Alphavirus mayaro*) is a single-stranded positive-sense RNA (ssRNA+) arbovirus, that belongs to the *Togaviridae* family and the genus *Alphavirus* [4]. The viral genome encodes MAYV structural proteins (CP, E3, E2, 6k/TF, E1) and non-structural proteins (nsP1, nsP2, nsP3, nsP4), which are involved in virus replication and pathogenesis [5]. It was first described in Trinidad in 1954 [6], and since then, several localized outbreaks of MAYV have been reported, especially in northern region of Brazil, due to increased trade and climate changes [1].

MAYV is the etiologic agent of Mayaro fever, a disease characterized by joint inflammation and arthralgias, which can progress to a chronic condition and cause clinical complications [7]. As an aggravating factor, there is no approved antiviral drug to treat Mayaro fever, and the treatment for the disease is based on controlling symptoms [4]. Another fact is that the virus is maintained in a wild enzootic cycle and the occurrence of spillover into the urban environment has drawn attention due to the potential to remain in an urban cycle [8,9].

On this basis, the emerging character of MAYV combined with the lack of antivirals to control infections caused by this pathogen demonstrates the need to search for molecules with the potential to treat the disease. In this context, drug repurposing can be an effective and rapid strategy to identify new indications of existing drugs to control virus spreading [10]. Rimantadine is an approved antiviral drug, which exhibits structural stability, good thermal and oxidative stability, extreme lipophilicity, and low consumption of energy [11]. In addition, it inhibits the influenza A virus by blocking the M2 ion channel, preventing viral uncoating, and its antiviral profile makes rimantadine an attractive candidate for drug repurposing [12].

Nevertheless, traditional antiviral assays based on viral antigens and/or plaque assays demonstrate low throughput, making it difficult to carry out larger-scale assays [13]. As a response, reporter viruses are an alternative system for high-throughput antiviral assays since the insertion of a specific reporter gene into the viral genome facilitates and provides a more efficient way of measuring viral replication, pathogenesis, and/or dissemination in infected cells and animals [14].

Previous investigations described the development and applicability of several viruses inserted with reporter genes, such as the Dengue virus [15], Influenza virus [16], Hepatitis C virus [17], Poxviruses [18], Sindbis virus, Chikungunya virus [19], and more recently, SARS-CoV-2 [20]. In a previous study, we also developed and characterized a stable enhanced green fluorescent protein (eGFP) reporter virus for the MAYV strain BeAr 20290, providing an interesting tool for antiviral screening assays [21]. Alternatively, Ramjag and coworkers described and characterized the MAYV expressing *nanoluciferase* (MAYV E2^{nLuc}) [22].However, both of these systems are based on the bacteriophage T7 and SP6 promoter, respectively [21,22], and therefore, depends on the transcription of backbone plasmid into infectious RNA to produce virions in eukaryotic cells [23,24]. This is an interesting technique; however, it presents limitations due to the instability of the RNA transfection into host cells, making it susceptible to degradation [25] In addition, the viral RNA can induce cellular immune response, compromising the efficient production of recombinant viruses and stimulating undesired mutations [26]. In contrast, cytomegalovirus (CMV) promoter-driven systems exhibit a less laborious and more efficient rescue process in eukaryotic cells, allowing transcription of the cDNA clone to be initiated directly by cellular RNA polymerase II (Chey et al., 2021). This system exhibits robust activity in mammalian cells, resulting in high levels of gene expression and increased production of viral particles [27]. In addition, it also presents higher accessibility, cost-effectiveness, and production speed than bacteriophage-driven systems, which makes it ideal for the efficient and economical production of viral vectors in research [28].

In this sense, we developed and characterized two stable infectious clones harbouring the *luciferase* reporters under the CMV promoter for antiviral screening assays, based on the strain BeAr 20290 of MAYV, Brazil [29]. The inserted reporter genes of *firefly luciferase (FLuc)* and *nanoluciferase (Nluc)* were designated as MAYV-*firefly* and MAYV-*nanoluc*, respectively. Additionally, we employed the system to identify Rimantadine hydrochloride (rtdH) as a repurposing drug, as well as validated MAYV-*nanoluc* as a tool as a powerful tool for high-throughput antiviral screening by using the compound EIDD-2749 (4′-Fluorouridine), which acts as an inhibitor of alphavirus RNA-dependent RNA polymerase [30]. Furthermore, rtdH presented a potential broad-spectrum activity by inhibiting the Zika virus (ZIKV).

2. Methods

2.1. Cells and compound

Vero E6 cells (kidney tissue derived from a normal adult African green monkey, ATCC E6) were cultivated on Dulbecco's Modified Essential Medium (DMEM, GIBCO) supplemented with 100 U/mL penicillin (Sigma-Aldrich), 100 mg/mL streptomycin (Sigma-Aldrich), 1 % (v/v) non-essential amino acids (Sigma-Aldrich) and 10 % (v/v) fetal bovine serum (FBS; Hyclone) at 37 °C in a humidified 5 % CO_2 incubator. Cell line was monthly tested to avoid mycoplasma infection.

The Rimantadine hydrochloride (rtdH, C12H22NCl, 99 %) was purchased from Sigma-Aldrich Laboratories and 4′-Fluorouridine (EIDD-2749, 98 %) was purchased from Cayman Chemical. The compounds were dissolved in DMSO (dimethyl sulfoxide), stored at −20 °C, and diluted in media at time of the assay.

2.2. Generation of the MAYV reporter construct

Using the previously constructed infectious cDNA clone of MAYV with the T7 promotor (termed as T7-MAYV) as a backbone (Li et al., 2019), the CMV-MAYV-*nanoluc* and CMV-MAYV-*firefly* were constructed under the control of the CMV promoter, in which a

cassette expressing the *NLuc* or/*FLuc* gene and a repeated sub-genomic (sg) promoter was inserted between the nonstructural nsP4 gene and the 5′-terminal of structural genes (Fig. 1). To achieve this, T7-MAYV-*nanoluc* was initially constructed and details for construction were as follows. Three individual fragments, respectively encompassing the sequences from part of nsp4 to the first sg promotor of the *NLuc* gene, and from the second sg promotor to the most of E1, were amplified and fused followed by pasting into the T7-MAYV backbone at *Eco*R I and Rsr II restriction sites to generate T7-MAYV-*nanoluc* clones. To facilitate the construction of the firefly reporter clone, *Asc*I and *Pac*I restriction sites were introduced at both ends of the *NLuc* gene, and the T7-MAYV-*firefly* clone was generated by replacing the *NLuc* gene of the T7-MAYV-*nanoluc* clone with *FLuc* through *Asc*I and *Pac*I sites. Then, the fragment encompassing the sequences from CMV promotor to nsp2 was obtained by fusion PCR and replace the corresponding part of T7-MAYV-*nanoluc* and T7-MAYV-*firefly* clones by *Bam*H I and Mlu restriction sites. The resulting plasmids were confirmed by sequencing and named as CMV-MAYV-*nanoluc* and CMV-MAYV-*firefly*. All primers used for PCRs were listed in Table 1, and the full-length sequences of the clones are available in Supplementary Material 1.

2.3. MAYV plasmids amplification and purification

Initially, 1 μg of the plasmids CMV-MAYV-*nanoluc* or CMV-MAYV-*firefly* was added to 200 μL of competent DH5-α Escheria coli and incubated on ice for 30 min. Subsequently, the bacteria were submitted to a thermal shock at 42 °C for 45 s, returned to ice for 2 min, and incubated with SOC medium at 37 °C for 1 h 200 rpm. Then, the DH5-α cells were streaked for isolation in solid Luria Berthani (LB) medium supplemented or not with Ampicillin (Sigma-Aldrich) at 50 μg/mL, for control based on the antibiotic resistance gene inserted in the plasmids. Afterward, the transformed bacteria were grown for 24 h and lysed to obtain the amplified plasmids. The purification process was performed by Plasmid Maxi kit (QUIAGEN) protocol, and the amount of DNA extracted was quantified through Nanodrop (Thermo Fisher).

2.4. MAYV infectious clone rescue

To produce the MAYV-*nanoluc* and MAYV-*firefly* virions, 1×10^6 BHK-21 cells/well seeded in 6 well plates were transfected with 5 μg of CMV-MAYV-*nanoluc* or CMV-MAYV-*firefly* plasmids using the LipofectamineTM LTX Reagent with PLUS Reagent (Thermo Fisher Scientific) and Optimem Medium following the manufacturer's instructions. After 48 h, the supernatant was collected and stored at −80 °C. The expression of *NLuc* and *FLuc* genes were assessed by luminescence reading on Glomax microplate reader (Promega), through the Renilla luciferase Assay System (Promega) or Luciferase Assay System (Promega), respectively, at different time-points post-transfection.

To determine viral titers, 8×10^4 Vero E6 cells/well were seeded in 24 wells plate, and 24 h later, the cells were infected with ten-fold serial dilutions of each MAYV infectious clone. Cells were incubated with viruses for 1 h at 37 °C and 5 % CO_2, followed by the inoculum removal, washes with PBS to remove the unbound virus, and addition of fresh medium supplemented with 1 % dilution of stock of penicillin and streptomycin, 2 % FBS, and 1 % carboxymethyl cellulose (CMC). Infected cells were incubated for 2 days in a humidified 5 % CO2 incubator at 37 °C, followed by fixation with 4 % formaldehyde and staining with 0.5 % violet crystal. The viral foci were visualized to determine plaque morphology. Images were analyzed at EVOs M5000 Cell Imaging Systems (Thermo Fisher Scientific).

All work was performed at biosafety level 2 under the authorization number SEI: 01245.006267/2022-14 CBQ: 163/02 from the CTNBio — National Technical Commission for Biosecurity from Brazil.

2.5. MAYV-nanoluc and -firefly growth kinetics

To assess the growth kinetics of both MAYV-*nanoluc* and MAYV-*firefly*, 1×10^5 Vero E6 cells were seeded in 12 well plates 24 h before infection. Later, cells were infected with MAYV wild-type strain BeAr 20290 ($MAYV_{WT}$), MAYV-*nanoluc*, or MAYV-*firefly* at the MOIs of 0.01, 0.05, and 0.1. After 2 h of incubation, the supernatants were removed, and cells were washed with PBS (1x) three times and replaced with fresh medium supplemented with 2 % FBS. At different time-points post-infection (4, 6, 12, 24, 36, and 48 h.p.i.), the culture medium was collected and stored at −80 °C.

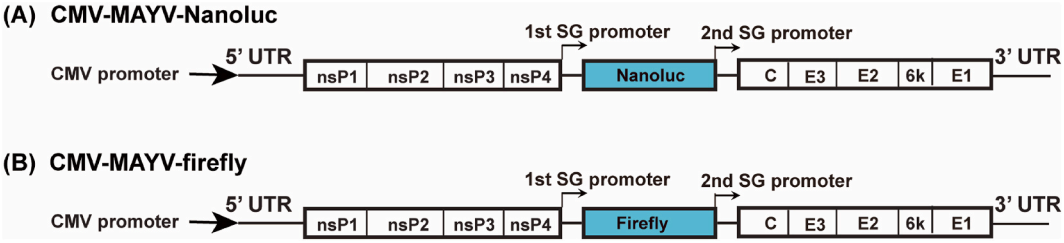

Fig. 1. Scheme of plasmid construction of MAYV-*nanoluc* and –*firefly*. The constructions were developed based on the sequence of MAYV BeAr 20290 strain, isolated in Brazil in 1960 from *Haemagogus* mosquitoes, belonging to genotype L. The marker genes that express the protein *Nano-luciferase* **(A)** and *Firefly luciferase* **(B)** were inserted in the viral genetic sequence between the non-structural proteins and capsid encoding genes.

Table 1
Primers used for construction of infectious MAYV reporter clones.

Primer	Sequence
*Eco*RI-MAYV nsp4-F	CCGGAATTCACAGAGAGCTGGTTCGCCGCC
Nanoluc-F	CTACACGACACCTATTCCACCCGGCGCGCCATGGTCTTCACACTCGAAGATTTC
Nanoluc-R	GGCGCGCCGGGTGGAATAGGTGTCGTGTAGAGCACCTATTTAGGACCGCC
MAYV-*Nanoluc*-Sg-Linker-F	ACGCATTCTGGCGTAATTAATTAATGTCATACATCTGTACGGCGGTCC
MAYV-*Nanoluc*-Sg-Linker-R	GTATGACATTAATTAATTACGCCAGAATGCGTTCGCACAGCCGCCAGCCGG
MAYV-E1-*Rsr*II	GGTCGGACCGGATTTGTCTGGATTATG
*Asc*I-*Firefly*-F	TTGGCGCGCCATGGAAGACGCCAAAAACATAAAG
*Pac*I-*Firefly*-R	TCCTTAATTAATTACACGGCGATCTTTCCGCCCTTC
CMV promoter-5′UTR-F	GCTCGTTTAGTGAACCGTATGGCGGGCAAGTGACAC
5′UTR + MAYV-nsp2-Mlu I–R	CG ACGCGTCAATAGGACATTGACGTGTT
*Bam*H I - CMV promoter-F	CGCGGATCC CATTGATTATTGACTAGTTA
CMV promoter-5′UTR-R	GTGTCACTTGCCCGCCATACGGTTCACTAAACGAGC

The viral titer of each time-point was determined by TCID50 (Median Tissue Culture Infectious Dose). To this, 5×10^3 Vero E6 cells were seeded in each well of a 96 well plate, were infected with ten-fold serial dilutions of the viral stocks, and incubated for 72 h at 37 °C, with 5 % CO2. Subsequently, viral titers were calculated according to the Spearman-Kärber algorithm as described by Killington and Hierholzer [31,32].

2.6. Stability of the reporter viruses in cell culture

To analyze whether the *FLuc* and *NLuc* reporter genes can be stably maintained after cell culture passaging, MAYV-*firefly* and MAYV-*nanoluc* were serially passaged in Vero E6 cells. For this, 1×10^6 cells were seeded in a T25 cm2 and infected with each MAYV infectious clone at an MOI of 0.1. Virus supernatant was stored at −80 °C, titrated through plaque reduction assay, and used to infect a new T25 cm2 flask using the same MOI. The cell passaging was performed 5 times. Additionally, the plaque focus was captured at EVOs M5000 Cell Imaging Systems (Thermo Fisher Scientific), and the morphology was compared among viruses.

To access the *luciferase* level expression during each passage, Vero E6 cells were seeded in a 48-well plate at a density of 2×10^4 cells per well and infected with each passage of the virus at an MOI of 0.1 for 24h. Afterward, cells were washed with PBS [1x] and harvested using Renilla-luciferase lysis buffer (Promega). Virus replication levels were quantified by measuring *NLuc* or *FLuc* activity through the Renilla luciferase assay system (Promega) or the Luciferase Assay System (Promega), respectively.

2.7. Determination of cytotoxic concentration of 50 % (CC_{50})

Cell viability was measured by the MTT [3-(4,5-dimethylthiazol-2-yl)-2,5-diphenyl tetrazolium bromide] (Sigma-Aldrich) assay as previously described [33,34]. Briefly, Vero E6 cells were plated to 24 well plates at a density of 8×10^4 cells/well for MAYV assays, or 5×10^3 cells/well in 96 well plate for ZIKV assays and incubated at 37 °C and 5 % CO_2. After 24h, medium containing two-fold serial dilutions of rtdH or EIDD-2749 (4′-Fluorouridine) was added to cells in concentrations ranging from 1.6 to 400 μM 1.56–200 μM, respectively. Since the CC50 was performed simultaneously with viral infection, the analysis for ZIKV was conducted after 72 h, and MAYV after 48 h. Then, the medium was replaced by MTT solution at 1 mg/mL for 30 min and replaced by 100 μL of DMSO (dimethyl sulfoxide) to solubilize the formazan crystals. The absorbance was measured at 490 nm on the Glomax microplate reader (Promega). Cell viability was calculated according to equation (T/C) × 100 %, where T and C represent the mean optical density of the treated and untreated control groups, respectively. The cytotoxic concentration of 50 % (CC_{50}) was calculated using GraphPad Prism 8.0.

2.8. Determination of effective concentration of 50 % (EC_{50}) using MAYV-nanoluc

To identify the effect of Rimantadine hydrochloride (rtdH) in MAYV replication, the MAYV-*nanoluc* was employed. To this, Vero E6 cells were plated in microplates of 48 wells at a concentration of 2×10^4 cells/well and incubated at 37 °C and 5 % CO_2 for 24 h. RtdH was diluted in a two-fold serial dilution following the concentrations of 1.6–400 μM, in the presence of the virus in a MOI of 0.1. The dose-response assay was also performed with EIDD-2749, a broad-spectrum inhibitor of alphaviruses (positive control) [30] in a two-fold serial dilution from 1.56 to 200 μM. After 24 h of incubation, the supernatant was removed, cells washed and lysed according to the Renilla Luciferase Assay System (Promega) kit protocol, and subsequently submitted to a luminescence analysis on the GloMax (Promega) plate reader. The effective concentration of 50 % inhibition (EC_{50}) was calculated using GraphPad Prism 8.0 software.

2.9. ZIKV assays

A wild-type ZIKV isolate from a clinical sample of a patient in Brazil ($ZIKV_{PE243}$) [35] was amplified employing infected Vero E6 cells in a 75 cm^2 flask for 3 days. It was produced, rescued, and titrated as previously described [34].

For determination of the EC50 using $ZIKV_{PE243}$, Vero E6 cells were seeded at a density of 5×10^3 cells per well into 96 well plates, infected with $ZIKV_{PE243}$ at a MOI of 0.01 and simultaneously treated with rtdH at concentrations ranging from 1.6 to 400 μM. For EC_{50},

cells were also. After 72 h, cells were fixed with 4 % formaldehyde, washed with PBS, and added of blocking buffer (BB) to perform an immunofluorescence assay [34]. The same protocol was performed in parallel in the absence of $ZIKV_{PE243}$ to determine CC50. The CC_{50} and EC_{50} were calculated using GraphPad Prism 8.0 software. These values were used to calculate the selectivity index ($SI = CC_{50}/EC_{50}$).

All work was performed at biosafety level 2 under the authorization number SEI: 01245.006267/2022-14 CBQ: 163/02 from the CTNBio — National Technical Commission for Biosecurity from Brazil.

2.10. Statistical analysis

Individual experiments were conducted in triplicates and all assays were performed a minimum of three times to confirm the reproducibility of the results. All data were normalized and expressed as mean and standard deviation. Differences between mean readings were compared using analysis of variance (one-way and two-way ANOVA) or Student's *t*-test, with p values < 0.05 considered

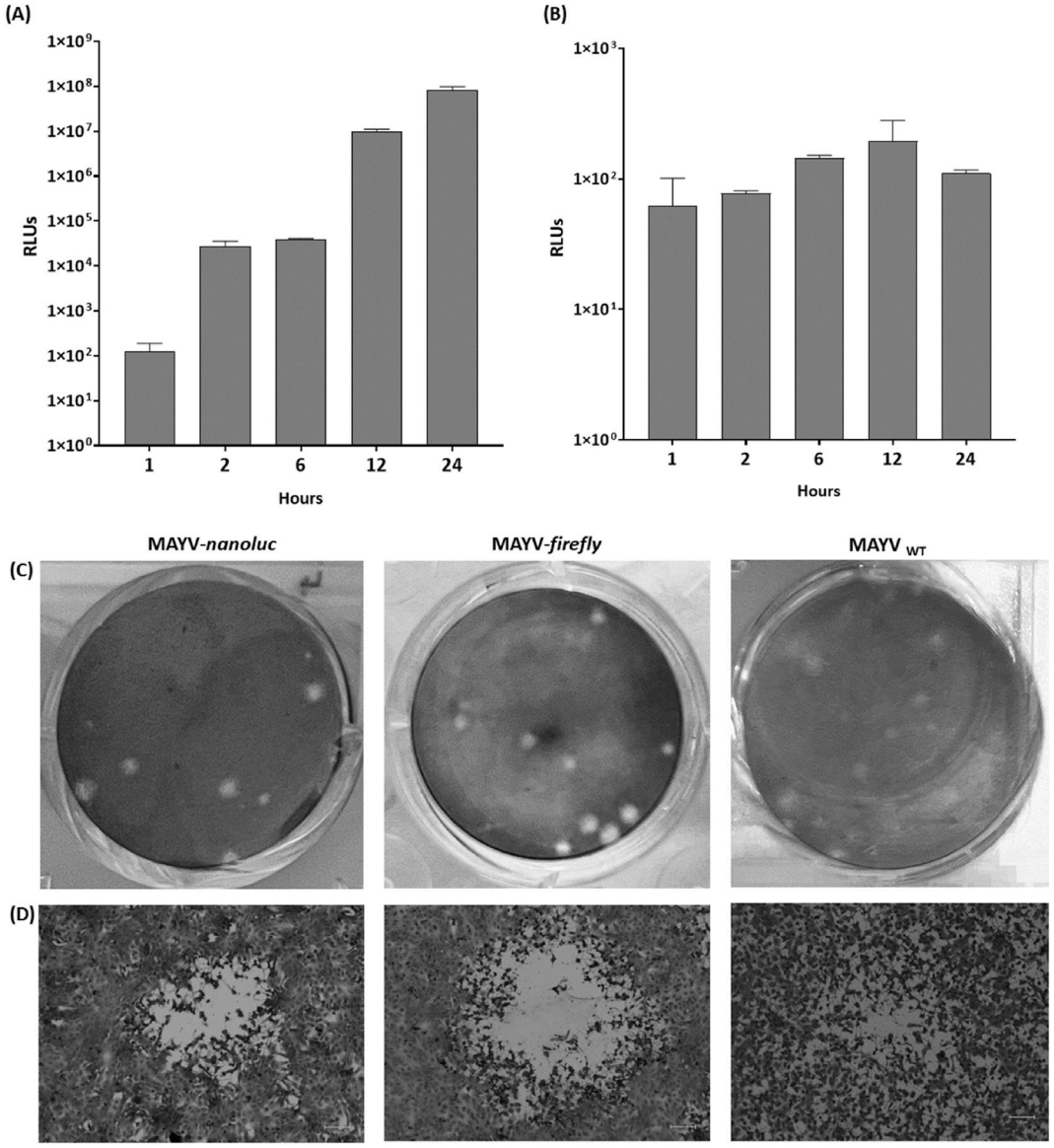

Fig. 2. Characterization of MAYV infectious clones. Analysis of luminescence expression in Vero E6 cells transfected with CMV-MAYV-*nanoluc* and CMV-MAYV-*firefly* and. Vero E6 cells were transfected with 1 μg of each plasmid and the expression of *Nanoluciferase* (A) and *Firefly luciferase* (B) were detected through Luciferase and *Renilla* luciferase assay system after transfection, respectively. (C) Plaque morphology of the recombinant viruses MAYV-*nanoluc* and MAYV-*firefly*, and the wild type. (D) Focus morphology of each virus in Vero E6 cells. Images were analyzed at EVOs M5000 cell imaging systems (Thermo Fisher Scientific). Scale bar 100 nm.

significant. GraphPad Prism 8.0 software was used to assess statistical differences of means of readings using a non-linear regression.

3. Results

3.1. Construction of MAYV-nanoluc and –firefly

To construct the cDNA clones of MAYV reporter viruses, we utilized the protocol reported to the construction of an eGFP Chikungunya reported in our previous study [36]. Briefly, a cassette expressing the *NLuc* or/*FLuc* gene and a repeated sub-genomic (sg) promoter was inserted between the nonstructural nsP4 gene and the 5′-terminal of structural genes. In addition, to avoid steps such as transcription to obtain viral RNAs in vitro, the reporter cDNA clones were placed under the control of CMV promotor (Fig. 1). The resulting plasmids were confirmed by sequencing and named as CMV-MAYV-*nanoluc* and CMV-MAYV-*firefly*.

3.2. Characterization and growth kinetics of MAYV-nanoluc and -firefly

The plasmids of CMV-MAYV-*nanoluc* and CMV-MAYV-*firefly* were transfected into Vero E6 cells to evaluate the efficacy of the infectious clone in producing an infectious particle. At different time points post-transfection, supernatants were collected and subjected to plaque assay to determine plaque morphology and virus production (Fig. 2). As shown in Fig. 2A, Relative Light Units (RLUs) were detectable at 1 h post-transfection (h.p.t.) for MAYV-*nanoluc* and increased until 24 h.p.t., reaching 1×10^8 RLUs (Fig. 2A). Alternatively, luminescence levels in cells transfected with MAYV-*firefly* were also detected 1 h.p.i., however, RLU values were maintained in about 1×10^2 RLUs until 24 h.p.t. (Fig. 2B).

After 48h, the supernatant of transfected cells was titrated employing the plaque formation assay, and as a result, the viral plaque morphology was homogeneously between $MAYV_{WT}$, MAYV-*nanoluc*, and *–firefly* (Fig. 2C). Visualization at a digital inverted microscope demonstrated that the MAYV-*nanoluc* and MAYV-*firefly* presented similar foci morphology, being those larger foci and with rounded edges when compared to $MAYV_{WT}$, which presented smaller and not defined foci (Fig. 2D).

Given the high stability and expression level of *luciferase* protein for both viruses at the first passage, we performed a growth kinetics comparison curve of the P1 from MAYV-*nanoluc*, *-firefly*, and $MAYV_{WT}$. To this, Vero E6 cells were infected with these three viruses at MOIs of 0.1, 0.05, and 0.01, and viral supernatant was collected at the time points 4, 6, 12, 24, 36, and 48 h.p.i. and titrated

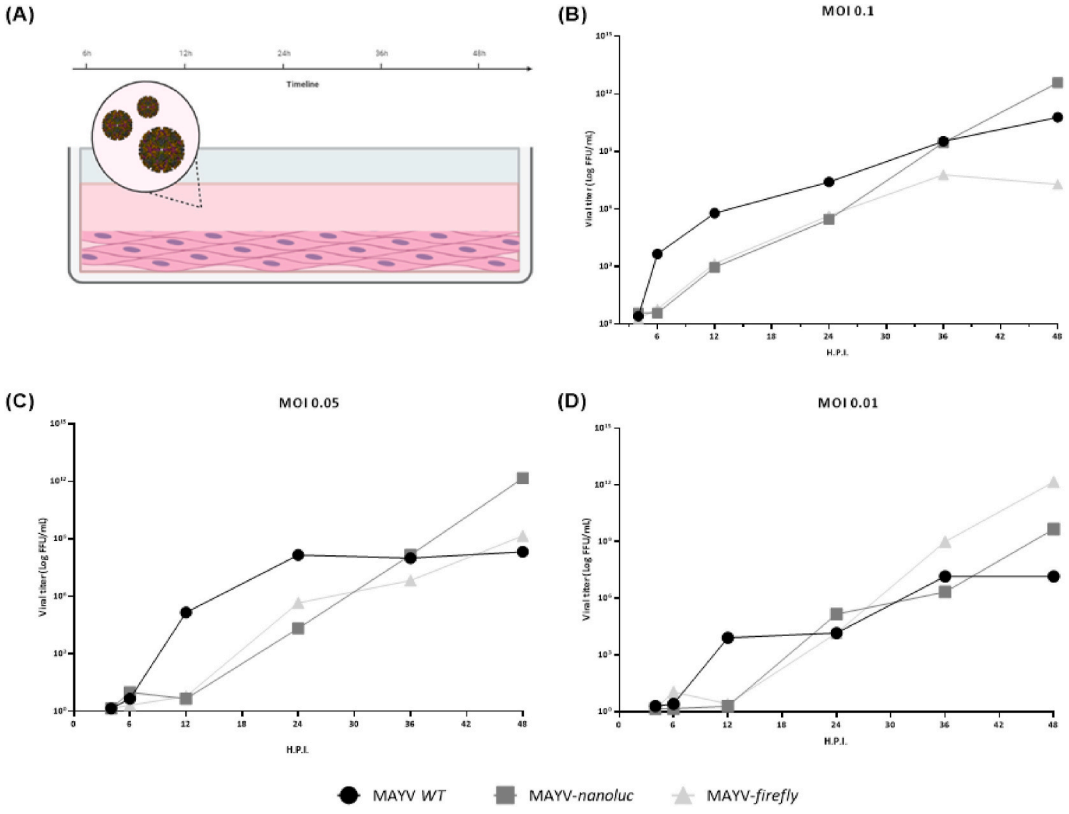

Fig. 3. Replication kinetics of MAYV in cell culture. (A) Schematic representation of replication kinetics assay. Growth kinetics of the wild type MAYV (indicated by ●), MAYV-*nanoluc* (indicated by ■), and MAYV-*firefly* (indicated by ▲). Vero E6 cells were infected with the three viruses at MOIs of 0.01 **(B)**, 0.05 **(C)**, and 0.1 **(D)**, viral supernatant was collected at different time points up to 48 h.p.i. and titrated by $TCID_{50}$.

by TCID50. As an outcome, the viral titers increased in a dose- and time-dependent manner (Fig. 3A). At all MOIs, both reporter viruses and $MAYV_{WT}$ presented low titers at 4 h.p.i., ranging between 1.45 and 3.88 pfu/mL (Fig. 3). At the MOIs of 0.1 (Figs. 3B) and 0.05 (Fig. 3C), the reporter viruses presented lower titers than the $MAYV_{WT}$ until 24h.p.i. However, MAYV-*nanoluc* reached a similar titer to $MAYV_{WT}$ at 36 h.p.i, presenting even higher titers than $MAYV_{WT}$ and MAYV-*firefly* at 48h.p.i. (Fig. 3B and C). Additionally, MAYV-*firefly* presented slightly higher titers than $MAYV_{WT}$ at the MOI of 0.05 at 48 h.p.i. (Fig. 3C). At the lowest MOI, MAYV-*nanoluc* presented higher titers than both MAYV-*firefly* and $MAYV_{WT}$ 24h.p.i., while MAYV-*nanoluc* and MAYV-*firefly* overcame $MAYV_{WT}$ titers at 48 h.p.i (Fig. 3D). These results demonstrated that the reporter viruses could efficiently replicate in Vero E6 cells, reaching similar growth rates to $MAYV_{WT}$.

3.3. *Nluc and Fluc reporter genes present different stability and luminescence expression levels in cell culture*

To analyze the in vitro stability and expression of the *FLuc* and *NLuc* genes, the viruses were serially passaged on Vero E6 cells for five times at an MOI of 0.1 for 48 h (Fig. 4A). The passages were titrated by plaque-forming assay, and the *luciferase* expression of each passage was measured by infecting Vero E6 cells with -*nanoluc*, at an MOI of 0.1 and MAYV-*firefly* at an MOI of 1, due to the contrast in the luminescence activity among the constructs. As an outcome, MAYV-*nanoluc* showed strong and consistent luminescence signals until the third passage, indicating the *NLuc* gene was stable for a minimum of three passages of infectious virus (Fig. 4B). Differently, MAYV-*firefly* presented a significant decrease in luminescence signal from the first to the second passage, indicating the loss of the *FLuc* gene probably due to selective pressure (Fig. 4C). Despite the gradual loss of reporter gene expression, viral titers were stable during passaging, varying from 2.67×10^6 to 2×10^8 PFU/mL.

3.4. *Employing MAYV-nanoluc reporter virus to identify rtdH as a drug candidate to be repurposed against MAYV infections*

In order to validate the employment of MAYV reporter viruses as tools for antiviral screening, and considering the high stability and sensibility of *NLuc* for in vitro assays, we used this reporter virus to analyze the antiviral activity of rtdH on MAYV replication. Additionally, the potential of MAYV-*nanoluc* as a powerful tool for antiviral screening was validated by treating infected cells with EIDD-2749.

To this, Vero E6 cells were infected with MAYV-*nanoluc* and treated with rtdH or EIDD-2749 for 24h. Afterward, the cells were lysed and subjected to a luminescence analysis to evaluate the reporter gene expression. Cell viability assay was performed in parallel. As a result, rtdH had an EC_{50} of 88.5 μM and a CC_{50} of 291.9 μM. Further, EIDD-2749 inhibited MAYV-*nanoluc* replication with an EC_{50} of 2.76 μM and CC_{50} of 4.99×10^7 μM. The calculated selectivity index ($SI = CC_{50}/EC_{50}$) for rtdH and EIDD-2749 were 2.3 and 1.8×10^7, respectively (Fig. 5). These results indicated that the MAYV-*nanoluc* reporter virus could be a useful tool for the evaluation of compounds presenting an anti-MAYV activity.

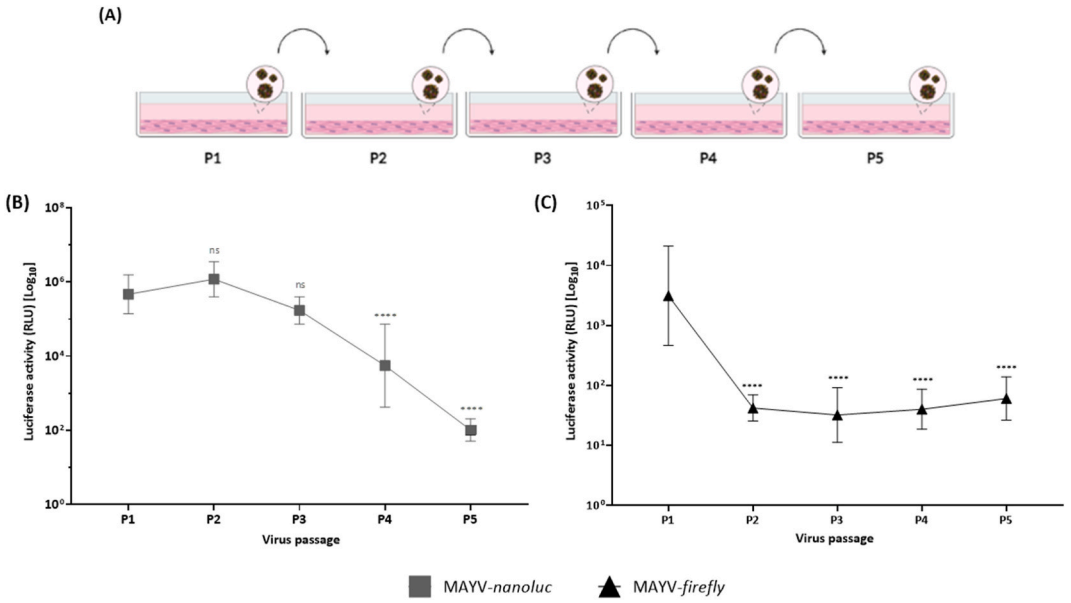

Fig. 4. Stability of the MAYV-*nanoluc* and -*firefly* viruses in cell culture. The *luciferase* expression of the different passages of MAYV-*nanoluc* **(A)** and –*firefly* **(B)** in Vero E6 cells. Vero E6 cells were serially infected with viruses for five passages. Viruses from each passage (P1–P5) were used to infect 1×10^5 Vero E6 cells at an MOI of 0.1, and the expression of *luciferase* proteins were detected 48 h.p.i. through *Luciferase* and *Renilla luciferase* assays, respectively. Mean values of three independent experiments each measured in triplicate including the standard deviation are shown. P values < 0.05 were considered significant. (**) $P < 0.01$, (***) $P < 0.001$ and (****) $P < 0.0001$.

3.5. RtdH also presents antiviral activity against ZIKV

The results presented here suggested that rtdH exerts its antiviral function against MAYV with a SI of 2.3, and, recently, it was described to possess activity against CHIKV [37]. Therefore, this drug could also present an antiviral activity on other arboviruses. To further investigate its broad-spectrum activity, we evaluated the inhibitory effects of rtdH on ZIKV replication. To this, Vero E6 cells were treated with the compound in a two-fold serial dilution ranging from 1.5 to 400 μM, along with the infection with $ZIKV_{PE243}$ at an MOI of 0.01 for 72h, when immunofluorescence assay was performed [34] (Fig. 6A). The results demonstrated that rtdH was able to inhibit ZIKV infection in a dose-dependent manner. The EC_{50} calculated by fluorescence value reduction was 80.3 μM and the CC_{50} of 194.3 μM, with an SI of 2.4 (Fig. 6B). Taken together, our findings demonstrate that rtdH presented an interesting antiviral effect against MAYV and ZIKV infections in vitro.

4. Discussion

The use of infectious clones of emergent viruses has been increasing in the past few years [13]. The insertion of specific reporter genes into the viral genome is a powerful tool to monitor the viral replication into infected mammalian cells, for applications such as high-throughput screening (HTS) for antiviral drug discovery [38]. Traditional plaque reduction assay for antiviral screening requires weeks to complete, while infectious clones expressing reporter genes can be done in days [39].

Here, we described the development of two DNA-launched replicative efficient MAYV-*luciferase* systems, expressing *NLuc* and *FLuc* genes. The *NLuc* or *FLuc* gene was inserted between the nonstructural nsP4 gene and the 5′-terminal of structural genes, and expressed under the control of sg promotor. Transfection of Vero E6 cells with the CMV-MAYV-*nanoluc* and –*firefly* plasmids resulted in detecting luminescence from the l*uciferase* reporters. The reporter viruses were infectious to Vero E6 cells, with robust *luciferase* levels production. While MAYV-*nanoluc* maintained the *NLuc* gene expression for three passages, MAYV-*firefly* was able to maintain the reporter gene for only one passage. Compared with the wild-type virus, the viral-growth kinetics were similar for both clones, showing indistinguishable replication efficiency. Additionally, we confirmed the usefulness of the MAYV-*nanoluc* for rapid antiviral screening assay using the Rimantadine hydrochloride, a well-known antiviral agent against the Influenza A virus. The broad-spectrum antiviral properties of rtdH were also demonstrated against ZIKV.

While the *FLuc* gene has more than 1.6 kb and encodes a 61 kDa protein, the *nLuc* gene has about three times fewer base pairs that encode a 19 kDa protein, being considered to present higher sensitivity and luminescent signal than *FLuc* [40]. In previous studies,

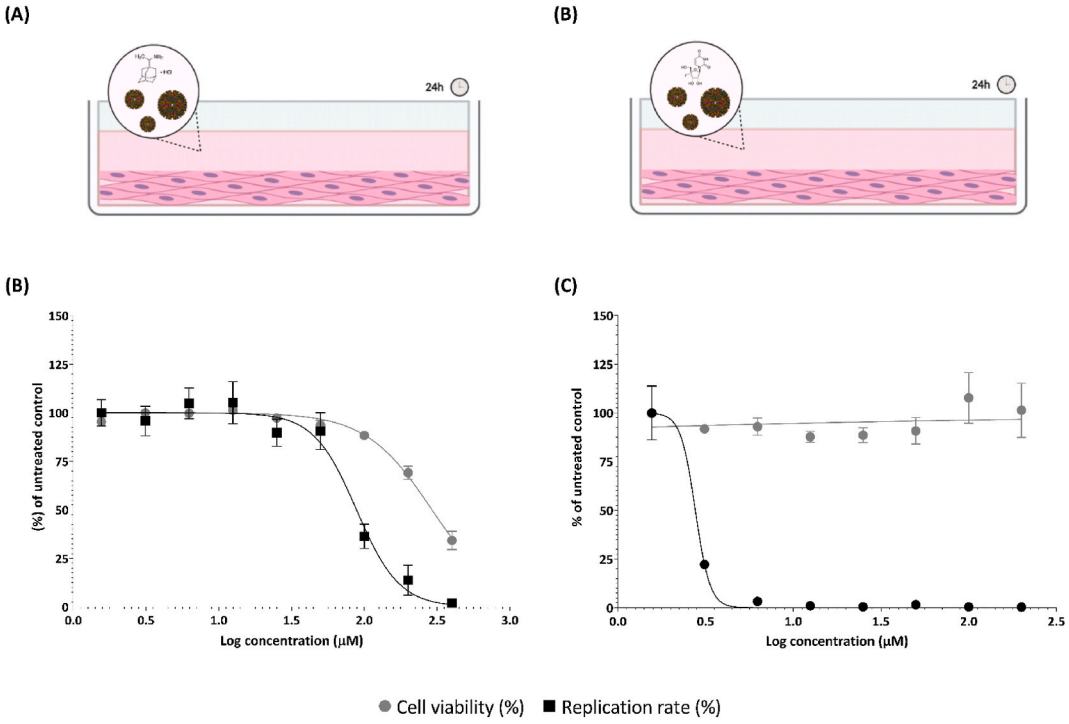

Fig. 5. Antiviral activity of Rimantadine hydrochloride on MAYV infectious clone. (A) Schematic representation of MAYV-*nanoluc* assay. Vero E6 cells were infected with MAYV-*nanoluc* at a MOI of 0.01 and treated with two-fold serial dilutionss of rtdH (1.6–400 μM) **(B)** or EIDD-2749 (1.56–200 μM) **(C)** for 24 h, when luminescence levels were measured by *Renilla* luciferase assay (indicated by ■) and cellular viability measured using MTT assay (indicated by ●). The effective concentration of 50 % (EC_{50}) and cytotoxic concentration of 50 % (CC_{50}) were determined. Mean values of three independent experiments each measured in quadruplicate including the standard deviation are shown.

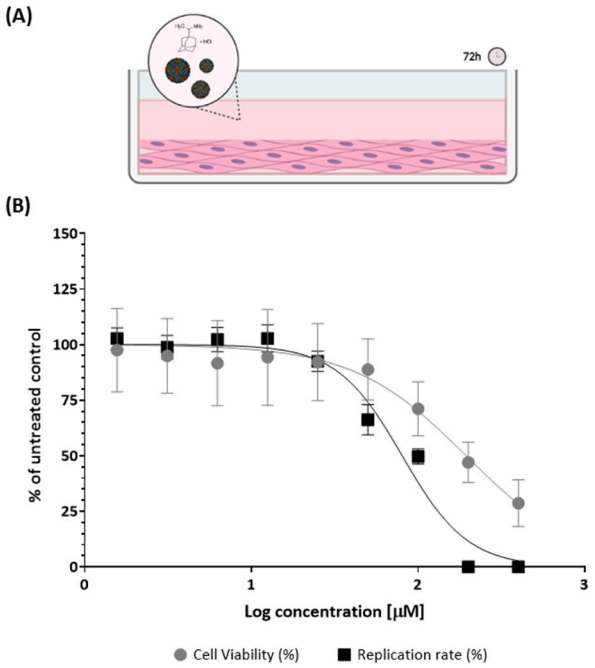

Fig. 6. Anti-ZIKV activity of Rimantadine hydrochloride. (A) Schematic representation of $ZIKV_{PE243}$ assay. **(B)** Vero E6 cells were treated with rtdH at concentrations ranging from 1.6 to 400 μM and the effective concentration of 50 % (EC_{50}) and cytotoxic concentration of 50 % (CC_{50}) were determined. ZIKV replication was measured by FFU/mL (indicated by ■) and cellular viability measured using MTT assay (indicated by ●). Mean values of three independent experiments each measured in triplicate including the standard deviation are shown.

constructs of the Sindbis virus (SINV) that presented the insertion of *FLuc* or *NLuc* genes, demonstrated different stability after cell passaging. In agreement with our data, the *NLuc* gene presented gene stability in SINV for ten passaging rounds, while the *FLuc* gene expression was only detected until the third passage [19]. Furthermore, in our study, the virus passages were performed in Vero E6 cells, which lack innate immune defenses and offer the potential for virus genetic drift, which possibly could also favor the loss of reporter genes during passaging [41].

Nevertheless, the *FLuc* system is applied *in vivo* due to the free diffusion of Firefly *luciferase* protein across the cell membrane [42]. *FLuc* possesses stable glow kinetics in the presence of its substrate and presents longer periods of photon emission than the *nano-luciferase* protein [43]. However, the *Fluc* gene presented low stability in MAYV infectious clones and was lost after the first passage, equivalent to about 4–6 rounds of virus infection [44]. This instability limits the utility of the *FLuc* marker for long-term studies or multiple rounds of viral replication, making it unsuitable for antiviral screening assays. Additionally, the bioluminescent activity of *FLuc* and *NLuc* originated through the reaction with different substrates that do not show cross-reactivity. In this sense, the systems can be applied concurrently for *in vivo* and in vitro dual bioluminescence analyses, allowing the simultaneous characterization of two different organisms or two separate biological processes [45].

Recently, our group pointed out rtdH as an inhibitor of CHIKV, an arbovirus that belongs to the same family and genus as MAYV, demonstrating promising results [37]. We proposed that the compound exhibits multiple effects on CHIKV, impairing mostly the early stages of the viral cycle, due to a virucidal action that involves viroporin blocking and interaction with the virus envelope [37]. Here, we described the antiviral properties of rtdH on both MAYV and ZIKV infections, presenting a SI of 2.3 and 2.4, respectively. In this sense, considering that rtdH has a known pharmacological profile and is an approved drug to treat Influenza A infection, it could be further evaluated in pre-clinical studies as a drug to be repurposed against MAYV, CHIKV and ZIKV infections, being applied more quickly than novel antivirals. Additionally, it could be used as a template to develop more potent drugs against MAYV, CHIKV and ZIKV infections. However, further studies are necessary to elucidate the mechanism of action on MAYV and ZIKV viroporins, which can be hypothesized by the differences between their structure and distribution in host cells. In addition, the compound EIDD-2749, previously described as RNA-dependent RNA polymerase (RdRp) inhibitor against MAYV [30] was used to validate MAYV-*nanoluc* as a potent tool for antiviral screening, presenting a SI of 1.8×10^7, in agreement with the previously published data. In summary, the results with rtdH and EIDD-2749 demonstrate that MAYV-*nanoluc* is a useful tool for HTS assays to detect inhibitors in different compound libraries for future antiviral research.

5. Conclusion

Considering the data described here, the reverse genetic system for MAYV employing DNA-launched plasmids containing *NLuc* and *FLuc* reporter genes were efficiently rescued and presented efficient replication as the wild-type virus in Vero E6 cells. Due to the high

stability of MAYV-*nanoluc* activity, which accurately represents virus replication rates, it is an applicable tool for antiviral assays that could facilitate the antiviral screening for novel anti-MAYV agents. Furthermore, we highlight the repurposing potential of Rimantadine hydrochloride as a broad-spectrum antiviral drug against MAYV and ZIKV.

Data availability statement

All data generated or analyzed during this study are included in this article.

CRediT authorship contribution statement

Mikaela dos Santos Marinho: Formal analysis, Investigation, Methodology, Validation, Writing – original draft. **Ya-Nan Zhang:** Investigation, Methodology, Writing – original draft. **Natasha Marques Cassani:** Investigation, Methodology, Writing – original draft, Writing – review & editing. **Igor Andrade Santos:** Investigation, Methodology, Writing – original draft, Writing – review & editing. **Ana Laura Costa Oliveira:** Investigation. **Anna Karla dos Santos Pereira:** Resources, Writing – review & editing. **Pedro Paulo Corbi:** Resources, Writing – review & editing. **Bo Zhang:** Methodology, Resources, Writing – review & editing. **Ana Carolina Gomes Jardim:** Funding acquisition, Supervision, Writing – review & editing.

Declaration of competing interest

The authors declare that they have no known competing financial interests or personal relationships that could have appeared to influence the work reported in this paper.

Acknowledgments

ACGJ is grateful to FAPEMIG (Fundação de Amparo à Pesquisa do Estado de Minas Gerais — Minas Gerais Research Foundation APQ-01487-22 and APQ-04686-22), and CAPES (Coordenação de Aperfeiçoamento de Pessoal de Nível Superior — Coordination of Superior Level Staff Improvement — Brasil —Prevention and Combat of Outbreaks, Endemics, Epidemics and Pandemics — Finance Code #88881.506794/2020-01 and — Finance Code 001). MDSM is grateful to FAPEMIG for scholarship #12152. NMC is grateful to CAPES for scholarship #88887.703845/2022-00. IAS thanks CNPq (Conselho Nacional de Desenvolvimento Científico e Tecnológico — National Council for Scientific and Technological Development 409187/2023-2) for scholarship #142495/2020-4, as well as for the CAPES.PrInt-UFU sandwich scholarship #88887.700246/2022-00 and FAPEMIG for scholarship #67355. PPC thanks to FAPESP (Fundação de Amparo à Pesquisa do Estado de São Paulo — São Paulo Research Foundation 2018/12062-4 and 2021/10265-8) and to Cancer Theranostics Innovation Center, CancerThera, Centros de Pesquisa, Inovação e Difusão-CEPID.

Appendix A. Supplementary data

Supplementary data to this article can be found online at https://doi.org/10.1016/j.heliyon.2024.e33885.

References

[1] J.C. Semenza, J. Rocklöv, K.L. Ebi, Climate change and cascading risks from infectious disease, Infect. Dis. Ther. (2022), https://doi.org/10.1007/S40121-022-00647-3.
[2] A. Zaid, F.J. Burt, X. Liu, Y.S. Poo, K. Zandi, A. Suhrbier, S.C. Weaver, M.M. Texeira, S. Mahalingam, Arthritogenic alphaviruses: epidemiological and clinical perspective on emerging arboviruses, Lancet Infect. Dis. 21 (2021) e123–e133, https://doi.org/10.1016/S1473-3099(20)30491-6.
[3] T.C. Pierson, M.S. Diamond, The continued threat of emerging flaviviruses, Nat Microbiol 5 (2020) 796–812, https://doi.org/10.1038/S41564-020-0714-0.
[4] R. Abdelnabi, S. Jacobs, L. Delang, J. Neyts, Antiviral drug discovery against arthritogenic alphaviruses: tools and molecular targets, Biochem. Pharmacol. 174 (2020), https://doi.org/10.1016/J.BCP.2019.113777.
[5] M. Bengue, A.R. Pintong, F. Liegeois, A. Nougairède, R. Hamel, J. Pompon, X. de Lamballerie, P. Roques, V. Choumet, D. Missé, Favipiravir inhibits mayaro virus infection in mice, Viruses 13 (2021) 2213, https://doi.org/10.3390/V13112213, 2213 13 (2021).
[6] C.R. Anderson, W.G. Downs, G.H. Wattley, N.W. Ahin, A.A. Reese, Mayaro virus: a new human disease agent. II. Isolation from blood of patients in Trinidad, B. W.I, Am. J. Trop. Med. Hyg. 6 (1957) 1012–1016, https://doi.org/10.4269/AJTMH.1957.6.1012.
[7] C.T. Diagne, M. Bengue, V. Choumet, R. Hamel, J. Pompon, D. Missé, Mayaro virus pathogenesis and transmission mechanisms, Pathogens 9 (2020) 738, https://doi.org/10.3390/PATHOGENS9090738, 738 9 (2020).
[8] Y. Acosta-Ampudia, D.M. Monsalve, Y. Rodríguez, Y. Pacheco, J.M. Anaya, C. Ramírez-Santana, Mayaro: an emerging viral threat? Emerg. Microb. Infect. 7 (2018) https://doi.org/10.1038/s41426-018-0163-5.
[9] S. Masmejan, D. Musso, M. Vouga, L. Pomar, P. Dashraath, M. Stojanov, A. Panchaud, D. Baud, Zika virus, Pathogens 9 (2020), https://doi.org/10.3390/pathogens9110898.
[10] L. Langendries, R. Abdelnabi, J. Neyts, L. Delang, Repurposing drugs for mayaro virus: identification of EIDD-1931, favipiravir and suramin as mayaro virus inhibitors, Microorganisms 9 (2021) 734, https://doi.org/10.3390/microorganisms9040734.
[11] K. Spilovska, F. Zemek, J. Korabecny, E. Nepovimova, O. Soukup, M. Windisch, K. Kuca, Adamantane – a lead structure for drugs in clinical practice, Curr. Med. Chem. 23 (2016) 3245–3266, https://doi.org/10.2174/0929867323666160525114026.
[12] J.C. Garcia, J.F. Justo, W.V.M. Machado, L.V.C. Assali, Structural, electronic, and vibrational properties of amino-adamantane and rimantadine isomers, J. Phys. Chem. A 114 (2010) 11977–11983, https://doi.org/10.1021/jp107496b.

[13] R.S. Fernandes, M.C.L.C. Freire, R. V Bueno, A.S. Godoy, L.H.V.G. Gil, G. Oliva, Reporter replicons for antiviral drug discovery against positive single-stranded RNA viruses, Viruses 12 (2020), https://doi.org/10.3390/v12060598.

[14] F. Kato, T. Hishiki, Dengue virus reporter replicon is a valuable tool for antiviral drug discovery and analysis of virus replication mechanisms, Viruses 8 (2016) 122, https://doi.org/10.3390/V8050122, 122 8 (2016).

[15] F. Pahmeier, C.J. Neufeldt, B. Cerikan, V. Prasad, C. Pape, V. Laketa, A. Ruggieri, R. Bartenschlager, M. Cortese, A versatile reporter system to monitor virus-infected cells and its application to Dengue virus and SARS-CoV-2, J. Virol. 95 (2021), https://doi.org/10.1128/JVI.01715-20/SUPPL_FILE/JVI.01715-20-S0003.MP4.

[16] A. Creanga, R.A. Gillespie, B.E. Fisher, S.F. Andrews, J. Lederhofer, C. Yap, L. Hatch, T. Stephens, Y. Tsybovsky, M.C. Crank, J.E. Ledgerwood, A.B. McDermott, J.R. Mascola, B.S. Graham, M. Kanekiyo, A comprehensive influenza reporter virus panel for high-throughput deep profiling of neutralizing antibodies, Nat. Commun. 12 (2021) 1–12, https://doi.org/10.1038/s41467-021-21954-2, 1 12 (2021).

[17] N.S. Eyre, A.L. Aloia, M.A. Joyce, M. Chulanetra, D.L. Tyrrell, M.R. Beard, Sensitive luminescent reporter viruses reveal appreciable release of hepatitis C virus NS5A protein into the extracellular environment, Virology 507 (2017) 20–31, https://doi.org/10.1016/J.VIROL.2017.04.003.

[18] Z. Bengali, P.S. Satheshkumar, B. Moss, Orthopoxvirus species and strain differences in cell entry, Virology 433 (2012) 506–512, https://doi.org/10.1016/J.VIROL.2012.08.044.

[19] C. Sun, C.L. Gardner, A.M. Watson, K.D. Ryman, W.B. Klimstra, Stable, high-level expression of reporter proteins from improved alphavirus expression vectors to track replication and dissemination during encephalitic and arthritogenic disease, J. Virol. 88 (2014) 2035–2046, https://doi.org/10.1128/JVI.02990-13/ASSET/FF4B8F21-19F2-4B43-95D3-6055AF65DF93/ASSETS/GRAPHIC/ZJV9990986550009. JPEG.

[20] K. Chiem, J.-G. Park, D. Morales Vasquez, R.K. Plemper, J.B. Torrelles, J.J. Kobie, M.R. Walter, C. Ye, L. Martinez-Sobrido, Monitoring SARS-CoV-2 infection using a double reporter-expressing virus, Microbiol. Spectr. 10 (2022), https://doi.org/10.1128/SPECTRUM.02379-22/SUPPL_FILE/REVIEWER-COMMENTS.PDF.

[21] X. Li, H. Zhang, Y. Zhang, J. Li, Z. Wang, C. Deng, A.C.G. Jardim, A.C.B. Terzian, M.L. Nogueira, B. Zhang, Development of a rapid antiviral screening assay based on eGFP reporter virus of Mayaro virus, Antivir. Res. 168 (2019) 82–90, https://doi.org/10.1016/J.ANTIVIRAL.2019.05.013.

[22] A. Ramjag, S. Cutrone, K. Lu, C. Crasto, J. Jin, S. Bakkour, C.V.F. Carrington, G. Simmons, A high-throughput screening assay to identify inhibitory antibodies targeting alphavirus release, Virol. J. 19 (2022) 170, https://doi.org/10.1186/s12985-022-01906-y.

[23] D. Fan, C. Hu, X. Yang, X. Yang, Y. Chen, J. Lin, Generation of a DNA-launched classical swine fever virus infectious clone packaged in bacterial artificial chromosome, Virus Res. 323 (2023) 198961, https://doi.org/10.1016/J.VIRUSRES.2022.198961.

[24] B.M. Kümmerer, in: Establishment and Application of Flavivirus Replicons, 2018, pp. 165–173, https://doi.org/10.1007/978-981-10-8727-1_12.

[25] G. Ávila-Pérez, A. Nogales, V. Martín, F. Almazán, L. Martínez-Sobrido, Reverse genetic approaches for the generation of recombinant Zika virus, Viruses 10 (2018) 597, https://doi.org/10.3390/v10110597.

[26] H. Zhang, D.K. Fischer, M. Shuda, P.S. Moore, S. Gao, Z. Ambrose, H. Guo, Construction and characterization of two SARS-CoV-2 minigenome replicon systems, J. Med. Virol. 94 (2022) 2438–2452, https://doi.org/10.1002/jmv.27650.

[27] T. Kurosaki, H. Nakamura, H. Sasaki, Y. Kodama, Suitable promoter for DNA vaccination using a pDNA ternary complex, Pharmaceutics 16 (2024) 679, https://doi.org/10.3390/pharmaceutics16050679.

[28] C.W. Tan, H.K. Tee, M.H.P. Lee, I.-C. Sam, Y.F. Chan, Enterovirus A71 DNA-launched infectious clone as a robust reverse genetic tool, PLoS One 11 (2016) e0162771, https://doi.org/10.1371/journal.pone.0162771.

[29] D.L.A. Espósito, B.A.L. da Fonseca, Complete genome sequence of mayaro virus (Togaviridae, alphavirus) strain BeAr 20290 from Brazil, Genome Announc. 3 (2015), https://doi.org/10.1128/genomeA.01372-15.

[30] P. Yin, N.A. May, L.S. Lello, A. Fayed, M.G. Parks, A.M. Drobish, S. Wang, M. Andrews, Z. Sticher, A.A. Kolykhalov, M.G. Natchus, G.R. Painter, A. Merits, M. Kielian, T.E. Morrison, 4′-Fluorouridine inhibits alphavirus replication and infection *in vitro* and *in vivo*, mBio (2024), https://doi.org/10.1128/mbio.00420-24.

[31] J. Hierholzer, R. Killington, Virology Methods Manual, 1996.

[32] J.F. Shimizu, S. Feferbaum-Leite, I.A. Santos, D.O.S. Martins, N.J. Kingston, M. Shegdar, C. Zothner, S.V. Sampaio, M. Harris, N.J. Stonehouse, A.C.G. Jardim, Effect of proteins isolated from Brazilian snakes on enterovirus A71 replication cycle: an approach against hand, foot and mouth disease, Int. J. Biol. Macromol. 241 (2023) 124519, https://doi.org/10.1016/J.IJBIOMAC.2023.124519.

[33] I.A. Santos, J.F. Shimizu, D.M. de Oliveira, D.O.S. Martins, L. Cardoso-Sousa, A.C.O. Cintra, V.H. Aquino, S.V. Sampaio, N. Nicolau-Junior, R. Sabino-Silva, A. Merits, M. Harris, A.C.G. Jardim, Chikungunya virus entry is strongly inhibited by phospholipase A2 isolated from the venom of Crotalus durissus terrificus, Sci. Rep. 11 (2021) 1–12, https://doi.org/10.1038/s41598-021-88039-4.

[34] N.M. Cassani, I.A. Santos, V.R. Grosche, G.M. Ferreira, M. Guevara-Vega, R.B. Rosa, L.J. Pena, N. Nicolau-Junior, A.C.O. Cintra, T.P. Mineo, R. Sabino-Silva, S. V. Sampaio, A.C.G. Jardim, Roles of Bothrops jararacussu toxins I and II: antiviral findings against Zika virus, Int. J. Biol. Macromol. 227 (2023) 630–640, https://doi.org/10.1016/j.ijbiomac.2022.12.102.

[35] C.L. Donald, B. Brennan, S.L. Cumberworth, V.V. Rezelj, J.J. Clark, M.T. Cordeiro, R. Freitas de Oliveira França, L.J. Pena, G.S. Wilkie, A. Da Silva Filipe, C. Davis, J. Hughes, M. Varjak, M. Selinger, L. Zuvanov, A.M. Owsianka, A.H. Patel, J. McLauchlan, B.D. Lindenbach, G. Fall, A.A. Sall, R. Biek, J. Rehwinkel, E. Schnettler, A. Kohl, Full genome sequence and sfRNA interferon antagonist activity of Zika virus from recife, Brazil, PLoS Neglected Trop. Dis. 10 (2016) e0005048, https://doi.org/10.1371/JOURNAL.PNTD.0005048.

[36] C.-L. Deng, S.-Q. Liu, D.-G. Zhou, L.-L. Xu, X.-D. Li, P.-T. Zhang, P.-H. Li, H.-Q. Ye, H.-P. Wei, Z.-M. Yuan, C.-F. Qin, B. Zhang, Development of neutralization assay using an eGFP Chikungunya virus, Viruses 8 (2016) 181, https://doi.org/10.3390/v8070181.

[37] I.A. Santos, A.K. dos S. Pereira, M. Guevara-Vega, R.E.F. de Paiva, R. Sabino-Silva, F.R.G. Bergamini, P.P. Corbi, A.C.G. Jardim, Repurposing potential of rimantadine hydrochloride and development of a promising platinum(II)-rimantadine metallodrug for the treatment of Chikungunya virus infection, Acta Trop. 227 (2022) 106300, https://doi.org/10.1016/j.actatropica.2021.106300.

[38] M.P. Jadhav, High-throughput screening (HTS) for the identification of novel antiviral scaffolds, Clin Pharmacol Drug Dev 3 (2014) 79–83, https://doi.org/10.1002/CPDD.99.

[39] J.Q. Li, C.L. Deng, D. Gu, X. Li, L. Shi, J. He, Q.Y. Zhang, B. Zhang, H.Q. Ye, Development of a replicon cell line-based high throughput antiviral assay for screening inhibitors of Zika virus, Antivir. Res. 150 (2018) 148–154, https://doi.org/10.1016/J.ANTIVIRAL.2017.12.017.

[40] C.G. England, E.B. Ehlerding, W. Cai, NanoLuc: a small luciferase is brightening up the field of bioluminescence, Bioconjugate Chem. 27 (2016) 1175–1187, https://doi.org/10.1021/ACS.BIOCONJCHEM.6B00112/ASSET/IMAGES/MEDIUM/BC-2016-00112G_0011.GIF.

[41] C. V Kuny, C.D. Bowen, D.W. Renner, C.M. Johnston, M.L. Szpara, In vitro evolution of herpes simplex virus 1 (HSV-1) reveals selection for syncytia and other minor variants in cell culture, Virus Evol 6 (2020), https://doi.org/10.1093/VE/VEAA013.

[42] J.E. Kim, S. Kalimuthu, B.C. Ahn, In vivo cell tracking with bioluminescence imaging, Nucl Med Mol Imaging 49 (2015) 3–10, https://doi.org/10.1007/S13139-014-0309-X/FIGURES/2.

[43] Y. Liang, P. Walczak, J.W.M. Bulte, Comparison of Red-Shifted Firefly Luciferase Ppy RE9 and Conventional Luc2 as Bioluminescence Imaging Reporter Genes for in Vivo Imaging of Stem Cells, 2012 016004, https://doi.org/10.1117/1.JBO.17.1.016004, 10.1117/1.JBO.17.1.016004 17.

[44] D.C. Mendonça, ErikV.S. Reis, NídiaE.C. Arias, H.J. Valencia, C.A. Bonjardim, A study of the MAYV replication cycle: correlation between the kinetics of viral multiplication and viral morphogenesis, Virus Res. 323 (2023) 199002, https://doi.org/10.1016/j.virusres.2022.199002.

[45] J. Czupryna, A. Tsourkas, Firefly luciferase and Rluc8 exhibit differential sensitivity to oxidative stress in apoptotic cells, PLoS One 6 (2011) e20073, https://doi.org/10.1371/JOURNAL.PONE.0020073.